MPI–PAE/PTh 17/90
April 1990

τ Decays to Pions

J. H. Kühn and A. Santamaria*

Max-Planck-Institut für Physik und Astrophysik
– Werner-Heisenberg-Institut für Physik –
P.O.Box 40 12 12, Munich (Fed. Rep. Germany)

ABSTRACT

Semileptonic τ decays to two and three pions are considered. Based on recent data for the pion form factor a new prediction for $\Gamma(\tau \to \nu\pi^-\pi^0)/\Gamma(\tau \to \nu e\bar{\nu}_e)$ of 1.32 ± 0.05 is derived. The chiral model — supplemented by vector dominace — is used to predict rate and differential distributions for the three pion mode in good agreement with present data. The parity violating asymmetry which has been predicted theoretically and observed experimentally is studied and found to be fairly insensitive towards the details of the model for the hadronic decays.

---

*On leave of absence from Departament de Física Teòrica, Universitat de València and IFIC, Universitat de València-CSIC, València, Spain.

1. Introduction

Semileptonic decays of the τ lepton have stimulated theoretical and experimental investigations since the discovery of the τ lepton [1, 2]. In particular decays to two and three pions — representing the strongest exclusive modes — have received considerable attention. The two pion, ρ-meson dominated mode serves as an excellent test of the CVC hypothesis and, on the basis of this assumption, can be predicted from the experimentally determined pion form factor [3, 4, 5]. The three pion mode, on the other hand, provides new information on the matrix element of the axial current. For low mass of the three pion system it allows to test the predictions based on chiral invariance [6, 7]. The distribution of the rate with respect to the mass of the hadronic system Q^2 allows to determine mass and width of the a_1 resonance and the dynamics of its decay. The three pion mode allows, furthermore, the construction of a parity violating asymmetry and thus the unambiguous determination of the magnitude and the sign of the ratio of the vector and axial couplings g_V/g_A at the lepton vertex.

With this motivation in mind a detailed analysis of the two and three pion channels has been performed. In chapter 2 the two pion channel is treated in some detail. The most recent experimental results, as compiled in Ref. 8 are incorporated. This leads to a prediction for $\Gamma_{2\pi}/\Gamma_e \equiv \Gamma(\tau \to \nu\pi^-\pi^0)/\Gamma(\tau \to e\nu\bar{\nu})$ of 1.32 ± 0.05 with a central value significantly higher than the previously quoted result [5] of 1.23 ± 0.12. This channel serves also as a testing ground for the ansatz of the ρ-propagator required for the 3π mode and for the detailed form of the a_1 Breit-Wigner amplitude. In particular the impact of an energy dependent width, the inclusion of a dispersive part and of higher radial excitations will be studied.

Chapter III is concerned with the analysis of the 3π decay. It is based on an amplitude derived [6] in the chiral limit, supplemented by vector dominance to correctly describe the resonances in the 2π and 3π mass distributions. Fixing the ρ propagator with the parameters adopted in chapter 2 to describe the pion form factor, the mass and width of the a_1 resonance are deduced from the 3π mass spectrum. The normalization of the rate is fixed unambiguously in this model. The dependence of the a_1 parameters, as deduced from the data, on the form of the resonance parametrization is studied. While the a_1 mass will turn out to be fairly insensive towards these details, the width will be significantly more model dependent.

Various spectra characterizing the distribution in the Dalitz plane are then calculated and compared with the experimental results, wherever available. These distributions can be predicted quite unambiguously and are in nice agreement with the data. The impact of the interference between the two ρ combinations on these distributions is stressed.

Motivated by the recent observation [9] of parity violation in τ decays as predicted in Ref. 7, the model dependence of the theoretical prediction is investigated. After a brief introduction of the kinematic variables relevant for this analysis the results derived from different models are presented. The differences are found to be small.

2. The two pion mode $\tau \to \nu\pi^-\pi^0$ and the pion form factor

Using the CVC hypothesis and isospin invariance, the decay rate relevant for $\tau \to \nu\pi^-\pi^0$ is expressed in terms of the pion form factor F through [3, 4]

$$\Gamma_{2\pi}/\Gamma_e = \frac{\cos^2\theta_c}{2}\int \frac{dQ^2}{m_\tau^2}\left(1-\frac{Q^2}{m_\tau^2}\right)^2\left(1+2\frac{Q^2}{m_\tau^2}\right)(1-\frac{4m_\pi^2}{Q^2})^{3/2}|F_{I=1}(Q^2)|^2 \quad (2.1)$$

where the subscript $I = 1$ indicates that the ω contribution has been subtracted. Various parametrizations have been suggested for $F(Q^2)$. They all incorporate $\rho-\omega$ mixing and an energy dependent width for the ρ, but differ in the exact functional dependence of $\Gamma_\rho(Q^2)$, in the incorporation of analyticity in the ρ propagator and in the inclusion of higher radial excitations ρ', ρ'' and eventually in a deformation of the resonance in the large Q^2 region as a consequence of the opening of a new channel.

Since a reliable parametrization of the ρ propagator will be needed for the a_1 decay amplitude in chapter 3, the maximum of information will be extracted from the presently available data on the pion form factor in the timelike region and the different choices will be confronted with the data . As a byproduct a new prediction for $\Gamma_{2\pi}/\Gamma_e$ will be derived.

The energy dependence of the resonance width is incorporated in the propagator through the substitution

$$i\ m_\rho \Gamma_\rho \Longrightarrow i\sqrt{Q^2}\Gamma_\rho(Q^2) \tag{2.2}$$

with

$$\Gamma_\rho(Q^2) = \Gamma_\rho \frac{m_\rho^2}{p_\rho^3}\frac{p^3}{Q^2} \tag{2.3}$$

and

$$2p = (Q^2 - 4m_\pi^2)^{1/2}; \quad 2p_\rho = (m_\rho^2 - 4m_\pi^2)^{1/2} \tag{2.4}$$

(Throughout this paper π^- and π^0 masses will be taken as 140 MeV). Such a form is expected from relativistic p-wave phase space and can be derived from the assumption of a constant $\rho\pi\pi$ coupling. It coincides with the functional dependence adopted by Gounaris and Sakurai (GS) [10] and also in Ref. 11, but differs from the one employed in Refs. 12, 13, 14. For the real part of the inverse propagator the expression $(m_\rho^2 - Q^2)$ can be adopted. This implies

$$BW^p(Q^2) = \frac{m_\rho^2}{m_\rho^2 - Q^2 - i\sqrt{Q^2}\Gamma_\rho(Q^2)} \tag{2.5}$$

Alternatively one may use the form proposed in Ref. 10. We repeat the derivation of the latter since a similar form will be used for the a_1. The real part of the inverse propagator is obtained from the requirement of analyticity combined with the proper subtractions to fix mass and width of the resonance and a normalization factor in the numerator to assure $BW(Q^2 = 0) = 1$. This leads to the following form of the Breit Wigner resonance:

$$BW^{GS}(Q^2) = \frac{m_\rho^2 + d\Gamma_\rho m_\rho}{m_\rho^2 - Q^2 + H(Q^2) - i\sqrt{Q^2}\Gamma_\rho(Q^2)} \tag{2.6}$$

with

$$H(Q^2) = \hat{H}(Q^2) - \hat{H}(m_\rho^2) - (Q^2 - m_\rho^2)\hat{H}'(m_\rho^2) \tag{2.7}$$

The function $\hat{H}$ can be obtained from $\sqrt{Q^2}\Gamma_\rho(Q^2)$ through a twice subtracted dispersion relation and is given by

$$\hat{H}(Q^2) = \frac{\Gamma_\rho m_\rho^2}{p_\rho^3}(Q^2/4 - m_\pi^2)h(Q^2)$$

with

$$h(Q^2) = \begin{cases} \frac{1}{2\pi}(1 - \frac{4m_\pi^2}{Q^2})^{1/2} \ln\left(\frac{1+(1-\frac{4m_\pi^2}{Q^2})^{1/2}}{1-(1-\frac{4m_\pi^2}{Q^2})^{1/2}}\right) & \text{if } 4m_\pi^2 \le Q^2 \\ \frac{i}{2\pi}(\frac{4m_\pi^2}{Q^2} - 1)^{1/2} \ln\left(\frac{i(\frac{4m_\pi^2}{Q^2}-1)^{1/2}+1}{i(\frac{4m_\pi^2}{Q^2}-1)^{1/2}-1}\right) & \text{if } 0 \le Q^2 \le 4m_\pi^2 \end{cases} \tag{2.8}$$

The constant

$$d = H(0)/(\Gamma_\rho m_\rho)$$

depends on m_ρ and m_π only. It is explicitly given by [10]

$$d = \frac{3}{2\pi}\frac{m_\pi^2}{p_\rho^2} \ln\left(\frac{m_\rho + 2p_\rho}{m_\rho - 2p_\rho}\right) + \frac{m_\rho}{2\pi p_\rho} - \frac{m_\pi^2 m_\rho}{\pi p_\rho^3} \tag{2.9}$$

As discussed in Ref. 8 the high Q^2 region (above $\sim$ 1 GeV) can only be described if either higher radial excitations like ρ' and ρ'' are included or if the high Q^2 region of the ρ resonance is significantly distorted due to the 4π and $\omega\pi$ threshold.

Parametrizing the form factor through

$$F(Q^2) = \left(BW_\rho \frac{1 + \alpha\ BW_\omega}{1+\alpha} + \beta\ BW_{\rho'} + \gamma\ BW_{\rho''}\right)/(1 + \beta + \gamma) \tag{2.10}$$

the free parameters are obtained from a χ^2 fit to the complete data set given in Ref. 8 and are listed in table 1 (models 1,2 for BW^P, models 4,5 for BW^{GS}). The masses and widths of the ω and the ρ'' have been fixed [15] to m_ω = 782 MeV, Γ_ω = 8.5 MeV, $m_{\rho''}$ = 1700 MeV, $\Gamma_{\rho''}$ = 235 MeV. A simple Breit Wigner with constant width has been used for the ω propagator. Consistent with Ref. 8 the relative phases of α, β and γ are assumed to be real. This leads in particular to a real pion form factor below threshold. Fits based on ρ and ω alone with propagators as given in eq. (2.5) or eq. (2.6) do not* lead to a satisfactory description of the data** as is evident from Fig. 1.

---

*We disagree with Ref. 11 in the applicability of a simple P-wave Breit-Wigner to the data. In fact the disagreement between model and data is evident already from their Fig. 2.

**For B_P and B_{GS} one finds m_ρ = 784 MeV, Γ_ρ = 127 MeV, χ^2/n_D = 1255/136 and m_ρ = 783 MeV, Γ_ρ = 139 MeV, χ^2/n_D = 640/136 respectively.

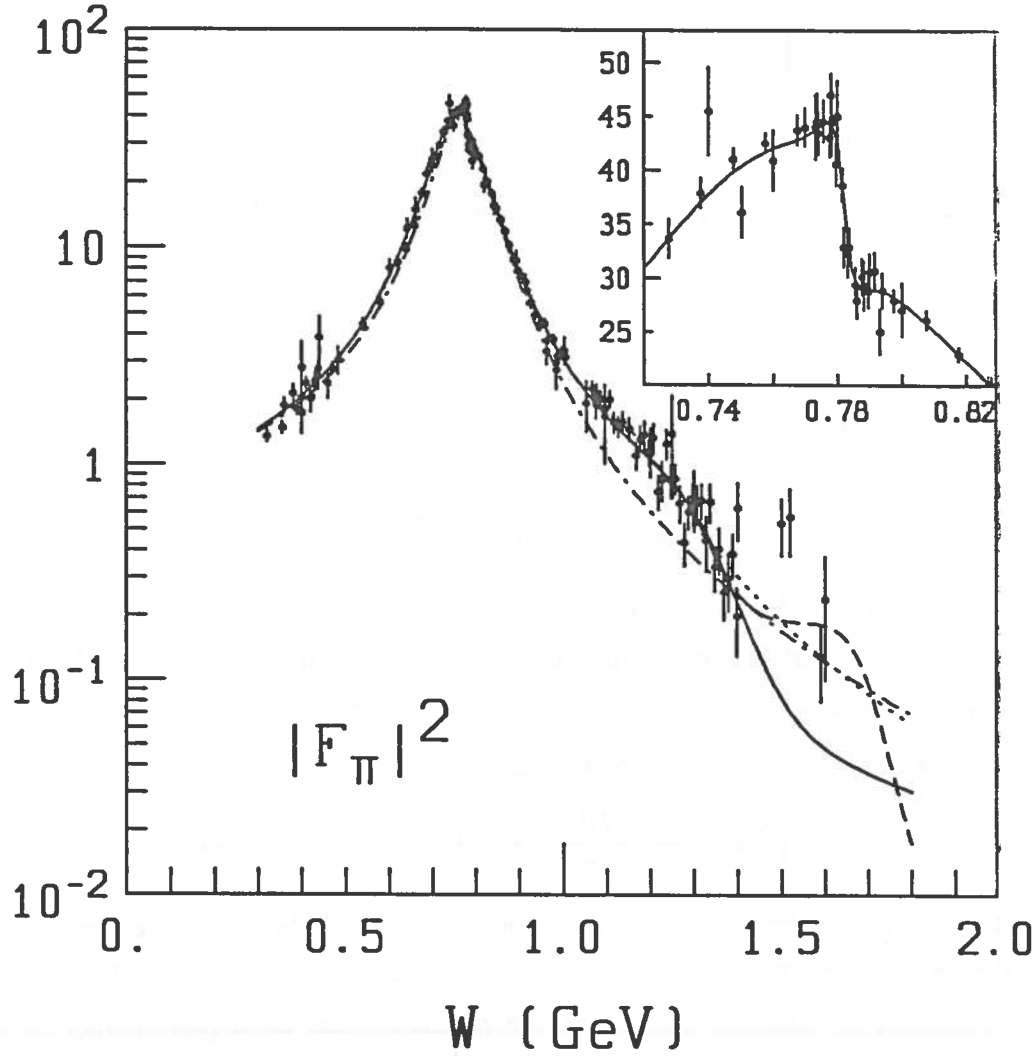

Fig. 1: Comparison of data [8] *and fits to the pion form factor, based on the Gounaris-Sakurai parametrization. Solid/dashed/dotted curves: models 4/5/6 from table 1. Dash-dotted curve: fit with* ρ *only and* $W = \sqrt{Q^2}$.

To detach ourselves from the assumption of higher radial excitations and to study the model dependence of the results for $\Gamma_{2\pi}/\Gamma_e$ the data were also fitted to the function [16]

$$F(Q^2) = BW_\rho \frac{1+\alpha\, BW_\omega}{1+\alpha} \times \begin{cases} \tilde{g}(Q^2) & \text{if } Q^2 > (m_\omega + m_\pi)^2 \\ \mathrm{Re}\,\tilde{g}(Q^2) & \text{if } Q^2 < (m_\omega + m_\pi)^2 \end{cases} \tag{2.11}$$

$$\tilde{g}(Q^2) = \left(\frac{m_0^2}{m_0^2 - Q^2 - i m_0 \Gamma_0}\right)^{n_0}$$

N	m_ρ	Γ_ρ	α	$m_{\rho'}$	$\Gamma_{\rho'}$	β	γ	m_o	Γ_o	n_o	χ^2/n_D	$\Gamma_{2\pi}/\Gamma_e$
1	773	145	$1.85 \cdot 10^{-3}$	1370	510	−0.145	$\equiv 0$	–	–	–	146/133	1.313
2	773	144	$1.84 \cdot 10^{-3}$	1320	390	−0.103	−0.037	–	–	–	136/132	1.314
3	774	143	$1.82 \cdot 10^{-3}$	–	–	–	–	1190	230	0.285	139/133	1.313
4	776	150	$1.95 \cdot 10^{-3}$	1370	350	−0.083	$\equiv 0$	–	–	–	159/133	1.320
5	776	151	$1.95 \cdot 10^{-3}$	1330	270	−0.052	−0.031	–	–	–	151/132	1.323
6	776	149	$1.94 \cdot 10^{-3}$	–	–	–	–	1180	105	0.142	141/133	1.323

Tab. 1: Results of fits to the pion form factor based on P-wave Breit-Wigner amplitudes (N=1,2,3) and on the Gounaris-Sakurai formula (N=4,5,6), excluding (N=1,4) or including (N=2,5) ρ'' or using the modification of eq. (2.11)*(N=3,6).*

The latter form will, however, not be used in the subsequent discussion of the three pion mode. The parameters resulting from this fit are also listed in table 1 (models 3 and 6). The curves based on the Gounaris-Sakurai amplitudes are shown in Fig. 1. Those based on the P-wave Breit-Wigner (2.5) are quite similar and are therefore not presented in the figure. Also shown in table 1 are the predictions for $\Gamma_{2\pi}/\Gamma_e$ based on (2.1). The ω contribution has been dropped in the evaluation of the integral, i.e. α has been set to 0. The result of 1.31-1.32 is fairly insensitive towards the details of the parametrization. The statistical error in the fitted parameters and in the resulting integral is small ($\lesssim 0.01$). The main uncertainty originates from the systematic error of the experiments (quoting between 2% and 4%) which leads to our final result of 1.32 with a conservative error estimate of ± 0.05. This result is above the previously quoted value [5] of 1.23 ± 0.12. One might expect some model dependence from the region with larger errors, i.e. above 1.0 GeV. This contribution is, however, rather small. Furthermore the fits are typically below the data points in this region, such that any model dependence would raise the prediction even further.

3. The three pion mode, chiral invariance and a_1 properties

3.1. General form of the amplitude

The three pion channel is entirely determined by the appropriate matrix element of the axial current J^A

$$\langle \pi^-(q_1)\pi^-(q_2)\pi^+(q_3)|J^A_\alpha(0)|0\rangle \equiv J_\alpha(q_1,q_2,q_3) \tag{3.1}$$

which implies a decay amplitude in the form

$$\mathcal{M} = \cos\theta_c \frac{G}{\sqrt{2}} \bar{v}_\nu(p_\nu)\gamma_\alpha(g_V - g_A\gamma_5)u_\tau(p_\tau)J^\alpha(q_1,q_2,q_3) \tag{3.2}$$

The standard model value $g_V = g_A = 1$ will be assumed in this chapter, the general form will be used in chapter 4. The most general ansatz of J_α for three pions in a spin 1 state which incorporates also the constraints from Bose symmetry reads

$$J_\alpha = F(s_1,s_2,Q^2)V_{1\alpha} + F(s_2,s_1,Q^2)V_{2\alpha} \tag{3.3}$$

$$V_{1\alpha} = q_{1\alpha} - q_{3\alpha} - Q_\alpha\frac{Q(q_1-q_3)}{Q^2}; \qquad V_{2\alpha} = q_{2\alpha} - q_{3\alpha} - Q_\alpha\frac{Q(q_2-q_3)}{Q^2}$$

with $s_1 = (q_2+q_3)^2$ etc.. It has been shown in Ref. 6 that form and normalization of J_α are fixed in the chiral limit

$$J_\alpha = -\frac{2\sqrt{2}i}{3f_\pi}(V_{1\alpha} + V_{2\alpha}) \tag{3.4}$$

with $f_\pi = 93.3$ MeV. It has been argued, furthermore [6, 7] that the correct distributions in the Dalitz plot are obtained once the enhancements from the ρ meson propagators are included along the prescription of vector dominance. In addition damping for large Q^2 is required which can be incorporated through a broad a_1 resonance. The normalization is still derived from eq. (3.4). One is thus led to the following amplitude*

$$J_\alpha = -i\frac{2\sqrt{2}}{3f_\pi}BW_a(Q^2)(B_\rho(s_2)V_{1\alpha} + B_\rho(s_1)V_{2\alpha}) \tag{3.5}$$

with the requirement $BW_a(Q^2) \underset{Q^2\to 0}{\longrightarrow} 1$ and $B_\rho(s_i) \underset{s_i\to 0}{\longrightarrow} 1$. The detailed forms of BW_a and B_ρ will be discussed below and will be based on the parametrizations used for the pion form factor.

---

*This amplitude has been discussed recently also by Pich [13]. We differ, however, in the form of the ρ and a_1 propagator and in the numerical result.

3.2. The spectral function and $d\Gamma/dQ^2$

The rate for Cabbibo allowed semileptonic τ decays can be expressed quite generally in terms of spectral functions ρ_0 and ρ_1, characterizing the relative amount of spin 0 and spin 1 hadronic final states [3, 4]

$$\Gamma_{3\pi}/\Gamma_e = \cos^2\theta_c 12\pi^2 \int \frac{dQ^2}{m_\tau^2}\Big(1-\frac{Q^2}{m_\tau^2}\Big)^2\Big(\rho_0(Q^2)+\Big(1+2\frac{Q^2}{m_\tau^2}\Big)\rho_1(Q^2)\Big) \tag{3.6}$$

with

$$\frac{1}{2\pi}\int \mathrm{dPS}(3\pi)\langle 0|J_\alpha^\dagger|3\pi\rangle\langle 3\pi|J_\beta|0\rangle = Q_\alpha Q_\beta \rho_0(Q^2) + (Q_\alpha Q_\beta - g_{\alpha\beta}Q^2)\rho_1(Q^2)$$

θ_c denotes the Cabbibo angle, dPS(3π) the Lorentz invariant phase space, Q the four momentum vector of the three-pion state and m_τ the τ-lepton mass.

From eq. (3.3) one derives $\rho_0 = 0$ and the spectral function ρ_1 can be cast into the form

$$\rho_1(Q^2) = \rho_{3\pi}(Q^2) = \frac{1}{6}\frac{1}{(4\pi)^4}\frac{8}{9f_\pi^2}|BW_a(Q^2)|^2 g(Q^2)/Q^2 \tag{3.7}$$

The three pion phase space factor*

$$g(Q^2) = \int \frac{ds_1 ds_2}{Q^2}\Big(-V_1^2|B_\rho(s_2)|^2 - V_2^2|B_\rho(s_1)|^2 - 2V_1V_2\,\mathrm{Re}\,B_\rho(s_1)B_\rho(s_2)^*\Big) \tag{3.8}$$

$$\begin{aligned} -V_1^2 &= (s_2-4m_\pi^2) + (s_3-s_1)^2/(4Q^2) \\ -V_2^2 &= (s_1-4m_\pi^2) + (s_3-s_2)^2/(4Q^2) \\ -V_1V_2 &= (Q^2/2 - s_3 - m_\pi^2/2) + (s_3-s_1)(s_3-s_2)/(4Q^2) \end{aligned} \tag{3.9}$$

replaces the relativistic P wave phase space which appeared in the two pion channel (eqs. (2.1, 2.3)). It has to be inserted also in the a_1 Breit Wigner, since — in analogy to the discussion in chapter 2 — $g(Q^2)$ governs also the a_1 decay rate. If a decay matrix element of the form

$$\mathcal{M}(a_1\to 3\pi) = f_a\varepsilon_a^\alpha\Big(B_\rho(s_2)V_{1\alpha} + B_\rho(s_1)V_{2\alpha}\Big) \tag{3.10}$$

---

*This form is closely related to formulas given in [17]. In fact $-V_1^2 = D(s_2, s_1)$, $-V_1V_2 = I(s_1, s_2)$, where D and I can be found in the $J^P = 1^+$ entry of table II in [17].

is assumed the decay rate reads

$$\Gamma(a_1 \to 3\pi) = \frac{1}{24m_a}\frac{f_a^2}{(4\pi)^3}g(m_a^2) \tag{3.11}$$

Special limiting cases which lead to simple analytic results for $m_\pi = 0$ are the narrow width approximation (without ρ' contribution)

$$g(Q^2) \underset{\Gamma_\rho \to 0}{\longrightarrow} \frac{2\pi m_\rho^3}{\Gamma_\rho}Q^2\left(\frac{m_\rho^2}{Q^2}(1-\frac{m_\rho^2}{Q^2}) + \frac{1}{12}(1-\frac{m_\rho^2}{Q^2})^3\right) \tag{3.12}$$

and the chiral limit

$$g(Q^2) \underset{Q^2 \to 0}{\longrightarrow} \frac{9}{16}Q^4 \tag{3.13}$$

We stress, that the squared matrix element is not a simple constant, such that $g(Q^2)$, even in the narrow width approximation, is not given by s-wave phase space and increases $\propto Q^2$.(This differs from the assumptions used in Ref. 18 where the corresponding function $-\operatorname{Im} C$ approaches a constant.) In analogy to the discussion in chapter 2 the parametrizations of both ρ and a_1 enhancements now have to be specified in detail.

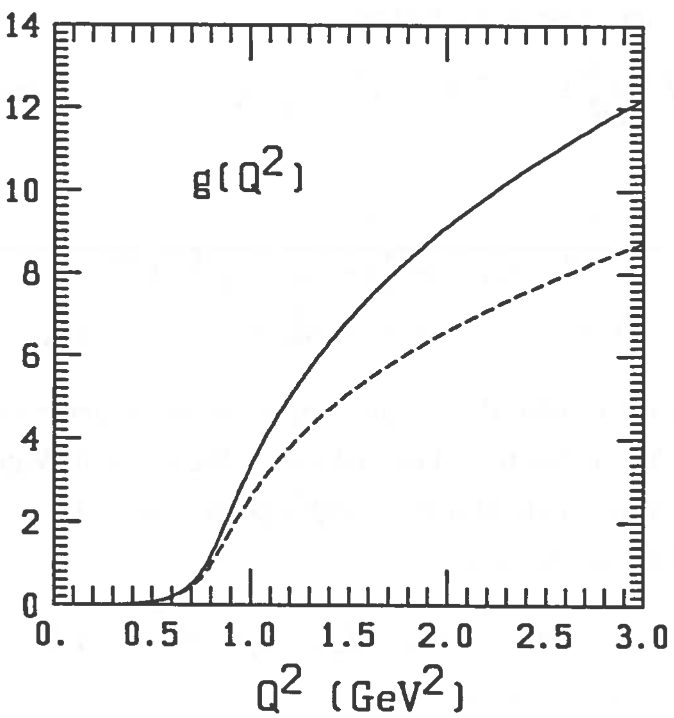

Fig. 2: Phase space function g for two choices of B_ρ. Solid curve: including ρ' (model 1); dashed curve: ρ only, with the same parameters.

A priori it is not evident that the ρ' (or ρ'') resonance contributes with the same relative strength to the a_1 decay and to the pion form factor. $g(Q^2)$ is therefore evaluated for the two possibilities of a single ρ contribution

$$B_\rho = BW_\rho^p \tag{3.14}$$

and ρ plus ρ'

$$B_\rho = (BW_\rho^p + \beta BW_{\rho'}^p)/(1+\beta) \tag{3.15}$$

(ρ parameters always taken from model 1 of table 1) with P-wave Breit Wigner amplitudes (Fig. 2). The main difference results from the factor $1/(1+\beta)$ in the normalization. The large s_1, s_2 region is strongly suppressed in the relevant integrals. Therefore the differential distributions differ barely for the two models and only the results from model 1 will be presented in section 3 below. A convenient parametrization of g for this model with ρ' only which is applicable in the region up to 3 GeV^2 reads (all parameters in appropriate powers of GeV):

$$g(Q^2) = \begin{cases} 4.1(Q^2 - 9m_\pi^2)^3(1 - 3.3(Q^2 - 9m_\pi^2) + 5.8(Q^2 - 9m_\pi^2)^2) & \text{if } Q^2 < (m_\rho + m_\pi)^2 \\ Q^2(1.623 + 10.38/Q^2 - 9.32/Q^4 + 0.65/Q^6) & \text{else} \end{cases} \tag{3.16}$$

The energy dependence of the imaginary part of the inverse a_1 propagator is fixed through

$$m_a\Gamma_a \Longrightarrow \sqrt{Q^2}\Gamma_a(Q^2) = m_a\Gamma_a \frac{g(Q^2)}{g(m_a^2)} \tag{3.17}$$

Two choices for the real part are suggested. One may either retain the form

$$BW_a(Q^2) = \frac{m_a^2}{m_a^2 - Q^2 - i\sqrt{Q^2}\Gamma_a(Q^2)} \tag{3.18}$$

which is choosen in analogy to the P-wave Breit Wigner for the ρ. The ARGUS result for the spectral function is shown in Fig. 3 together with the curve resulting from B_ρ chosen according to eq. (3.15). In table 2 the parameters of the fit are listed for both models (eqs. (3.14, 3.15)) without fixing the normalization and thus allowing for a scale factor S different from 1. Considering the present uncertainty in the rate*, satisfactory agreement is obtained for both models.

---

*We note that $B(\pi^-\pi^-\pi^+) = 5.6 \pm 0.7\%$ has been obtained in [19] whereas the present world average [15] amounts to $6.8 \pm .6\%$ with individual results ranging between 5.0 and 9.7%.

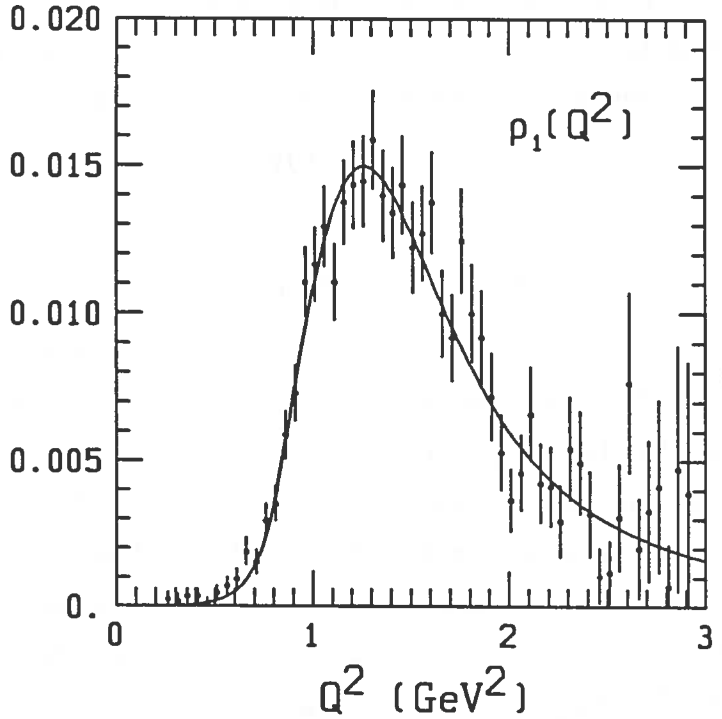

Fig. 3: Spectral function as derived from eq. (3.15) *(including the scale factor of 0.85) and data from Ref.* 19.

BW_a	B_ρ	Scale factor	m_a[MeV]	Γ_a[MeV]	χ^2/n_D	$\Gamma_{\pi^-\pi^-\pi^0}/\Gamma_e$ ($S \equiv 1$)
no dispersive correction	BW^p, no ρ'	1.06 ± 0.08	1246 ± 12	562 ± 38	48/51	0.286
no dispersive correction	BW^p, withρ'	0.85 ± 0.07	1251 ± 13	599 ± 44	52/51	0.356
with dispersive correction	BW^{GS}, no ρ'	0.48 ± 0.03	1252 ± 15	655 ± 56	65/51	0.622
with dispersive correction	BW^{GS}, with ρ'	0.43 ± 0.03	1255 ± 16	696 ± 66	71/51	0.705

Tab. 2: Results of the fits to the experimental data [19] *for the spectral function using theoretical predictions based on different assumptions for the ρ and a_1 enhancements.*

Alternatively one may incorporate a dispersive part

$$BW_a^{disp}(Q^2) = \frac{m_a^2 + d_a \Gamma_a m_a}{m_a^2 - Q^2 + H(Q^2) - i\sqrt{Q^2}\Gamma_a(Q^2)} \tag{3.19}$$

similar to the treatment of the ρ-propagator in Ref. 10. The function $H(s)$ is obtained from $g(s)$ through

$$\begin{aligned} H(Q^2) &= \frac{\Gamma_a m_a}{g(m_a^2)}\left[\hat{H}(Q^2) - \hat{H}(m_a^2) - (Q^2 - m_a^2)\hat{H}'(m_a^2)\right] \\ \hat{H}(Q^2) &= -\frac{1}{\pi}Q^4 \int \frac{ds'}{s'^2}\frac{g(s')}{s' - Q^2} \\ d_a &= \frac{-\hat{H}(m_a^2) + m_a^2 \hat{H}'(m_a^2)}{g(m_a^2)} \end{aligned} \tag{3.20}$$

The first subtraction assures the proper location of the a_1 mass, the second subtraction is required to allow the interpretation of Γ_a as width of the a_1. The additional term in the numerator assures the correct normalization in the chiral limit $Q^2 \to 0$. The dispersive integral in eq. (3.20) is ultraviolet convergent and has been evaluated numerically.

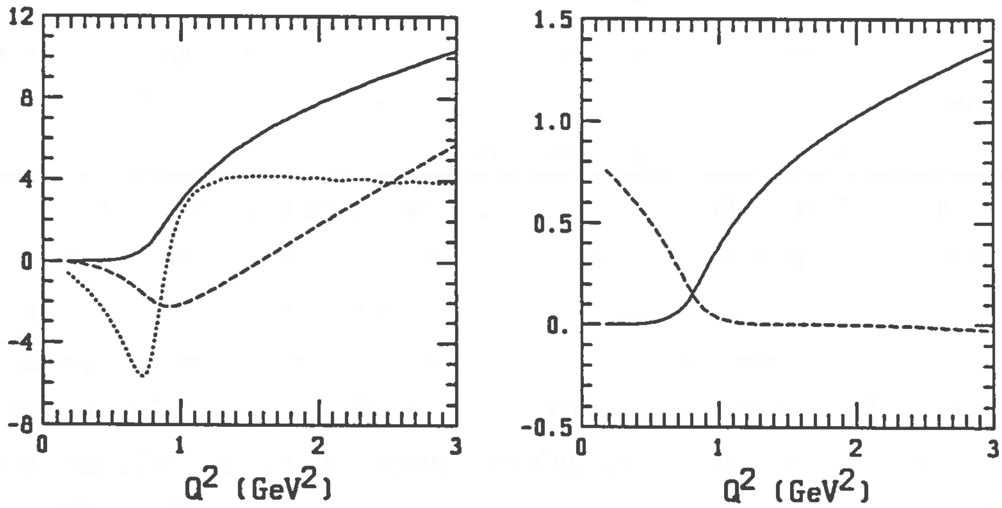

Fig. 4: a)The functions g, $\hat{H}$ and $\hat{H}'$ (solid/dashed/dotted curves) as defined in eq. (3.20) *(in units of* GeV^2*).*
b)The functions $H(Q^2)$ (dashed) and $\sqrt{Q^2}\Gamma_a(Q^2)$ (solid) (in units of GeV^2*) which modify the a_1 propagator with the a_1 parameters listed in table 2.*

The results for $g(Q^2)$, $\hat{H}(Q^2)$ and $\hat{H}'(Q^2)$ are shown in Fig. 4a based on

$$B_\rho = B_\rho^{GS}$$

(with ρ parameters taken from model 4 of Table 1), those for $H(Q^2)$ and $\sqrt{Q^2}\Gamma(Q^2)$ in Fig. 4b. Independent from differences in the detailed form of g resulting from differences in B_ρ one obtains a drastic change in the normalization $d \approx 1.$ $(1 + d_a\Gamma_a/m_a)^2 \approx 2!$). Thus this ansatz leads to a prediction of $\Gamma_{\pi^-\pi^-\pi^+}/\Gamma_e = 0.62$ which is about a factor 2 higher than the one discussed above. This seems to be incompatible with the present world average. Including the ρ' contribution increases the difference even further. Also the shape differs significantly from the case without the dispersive part. Even allowing for the scale factor listed in table 2 to adopt the normalization of the data, the shape of the spectral function is still not reproduced as well as in the previous case — a fact evident from table 2.

3.3. Distributions in the Dalitz plane.

While the distribution $d\Gamma/dQ^2$ is reproduced through the simple ansatz of an a_1 resonance and $\rho\pi$ phase space (see e.g. [12]) differential distributions should allow to test the model in more detail.

One characteristic feature is the interference between the two ρ combinations. This aspect (barely visible in $g(s)$ in Fig. 2) reflects itself in the mass distribution of like sign and opposite sign pion pairs.

In Fig. 5 $d\Gamma/d\sqrt{s}_1$ and $d\Gamma/d\sqrt{s}_3$ are shown with $\sqrt{s_1} = m(\pi^+\pi^-)$ and $\sqrt{s_3} = m(\pi^-\pi^-)$ integrated over all Q^2. (Note that every event enters twice in the distribution $d\Gamma/d\sqrt{s_1}$.) These curves are in nice agreement with the results from Ref. 19. The cross-over, however, of the two curves in the region of small s_1, s_3 is characteristic for the interference. It is not present in the case of incoherent superposition. This feature is absent in the published data of ARGUS [19] although the errors are still large. More recent data from the same experiment [20] and data from MAC [21] seem to indicate the presence of this effect.

Similar comparisons can be made for distributions in s_1 where s_2 has been integrated over the ρ band (0.5 GeV$^2 \leq s_2 \leq 0.7$ GeV^2), and Q^2 has been integrated over a fixed interval. Satisfactory agreement is obtained for shapes and normalization.

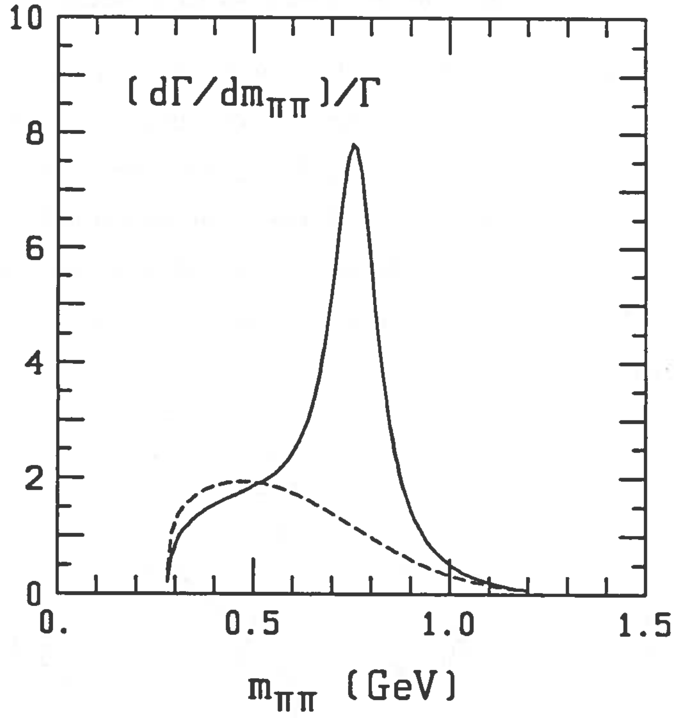

Fig. 5: Prediction for the mass distribution of like sign (dashed) and opposite sign (solid) (two entries per event) pion pairs.

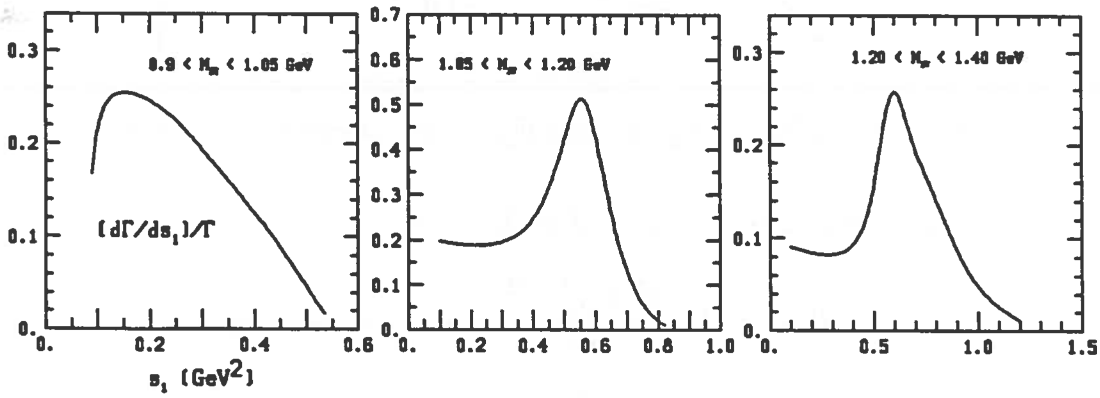

Fig. 6: Mass distribution of $\pi^+\pi^-$ after restricting the invariant mass of the second $\pi^+\pi^-$ combination to the ρ band (0.5 – 0.7 GeV^2). The prediction is given for restricted $Q^2 = M_{3\pi}^2$ intervals.

4. Parity violation in τ decays

It has been observed in Ref. 7 that the three pion mode can serve to establish parity violation in τ decays. For the sake of completeness the basic formulae and kinematic variables will be repeated. The model dependence will then be studied in some detail. The asymmetry will firstly be described in the case where both the τ and the 3π restframe can be reconstructed, relevant e.g. for a τ factory close to threshold. Then the case of the τ decaying in flight and resulting from e^+e^- annihilation will be studied.

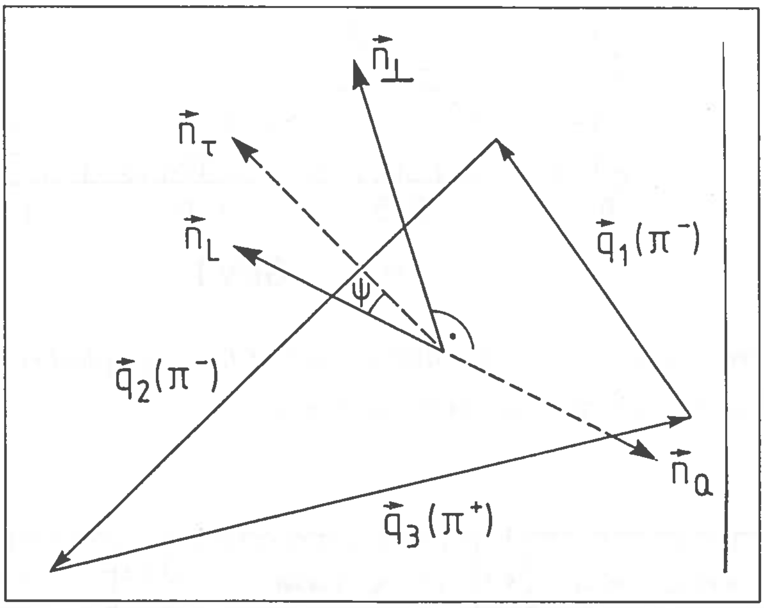

Fig. 7: Definition of $\vec{n}_\perp$, $\vec{n}_\tau$ and $\vec{n}_Q$ in the hadronic rest frame.

The differential rate is expressed in the form*

$$d\Gamma = \cos\theta_c \frac{(g_V^2 + g_A^2)G^2}{4m_\tau}\ \omega\ dPS(p_\tau; p_\nu, q_1, q_2, q_3) \tag{4.1}$$

with $\omega = \omega_{PC} + \omega_{PV}$. The parity violating piece is given by

$$\begin{aligned}\omega_{PV} &= \gamma_{VA} 2\,\mathrm{Im}\,\epsilon(p_\tau, J, J^*, p_\nu) \\ &= -\gamma_{VA} 12 \epsilon(q_1, q_2, q_3, p_\tau)\frac{8}{9f_\pi^2}|BW_a(Q^2)|^2\,\mathrm{Im}\,B_\rho(s_1)B_\rho(s_2)^*\end{aligned} \tag{4.2}$$

*In this paper we follow the conventions of Bjorken and Drell and use $\epsilon_{0123} = +1$.

$$= -\gamma_{VA} 3(\vec{n}_\perp \vec{n}_\tau)(m_\tau^2 - Q^2)\sqrt{(s_1 s_2 s_3 - m_\pi^2(Q^2 - m_\pi^2)^2)/Q^2} \times \frac{8}{9f_\pi^2}|BW_a(Q^2)|^2 \, \mathrm{Im}\, B_\rho(s_1)B_\rho(s_2)^*$$

where $\gamma_{VA} = 2g_V g_A/(g_V^2 + g_A^2)$ and $\vec{n}_\perp = \vec{q}_1 \times \vec{q}_2/|\vec{q}_1 \times \vec{q}_2|$ denotes the normal on the plane spanned by the momenta of the three pions in the rest frame of the hadronic system, $\vec{n}_\tau$ the direction of flight of the τ viewed from the rest frame of the hadronic system. (See Fig. 7)

The parity conserving part reads

$$\omega_{PC} = (m_\tau^2 - Q^2)\left[\frac{(m_\tau^2 - Q^2)}{Q^2}|\vec{n}_\tau \vec{J}|^2 + |\vec{J}|^2\right] \tag{4.3}$$

where $\vec{J}$ is to be taken in the 3π rest frame.

To extract the parity violating piece experimentally, two situations of practical interest may be considered:

Taus decaying at rest: This is equivalent to those situations in which the tau rest frame can be fully reconstructed. In this case $\vec{n}_\tau = -\vec{n}_Q$ (where $\vec{n}_Q$ denotes the direction of the hadrons in the lab system) is known and the first moment with respect to $(\vec{n}_\perp \vec{n}_\tau)\,\mathrm{sign}(s_1 - s_2)$ can be considered. The antisymmetric function $\mathrm{sign}(s_1 - s_2)$ is needed to avoid a null result due to the Bose symmetry of the amplidude. (For an alternative choice see [7] eq.4.6.) Using the factorization property of phase space

$$dPS(p_\tau; p_\nu, q_1, q_2, q_3) = \frac{dQ^2}{2\pi} dPS(p_\tau; p_\nu, Q) dPS(Q; q_1, q_2, q_3) \tag{4.4}$$

we can define the moments with respect to $(\vec{n}_\perp \vec{n}_\tau)\,\mathrm{sign}(s_1 - s_2)$ by integrating the three-pion phase space, keeping the direction of the hadronic system fixed:

$$\langle(\vec{n}_\perp \vec{n}_\tau)\,\mathrm{sign}(s_1 - s_2)\rangle \equiv \frac{\int dPS(Q; q_1, q_2, q_3)(\vec{n}_\perp \vec{n}_\tau)\,\mathrm{sign}(s_1 - s_2)\omega}{\int dPS(Q; q_1, q_2, q_3)\omega} \tag{4.5}$$

An explicit calculation gives

$$\langle(\vec{n}_\perp \vec{n}_\tau)\,\mathrm{sign}(s_1 - s_2)\rangle = -\gamma_{AV} A_{LR}(Q^2) \tag{4.6}$$

where A_{LR} depends on Q^2 only:

$$A_{LR}(Q^2) = \frac{3Q^2 \int ds_1 ds_2 \sqrt{(s_1 s_2 s_3 - m_\pi^2(Q^2 - m_\pi^2)^2)/Q^2}\,\mathrm{sign}(s_1 - s_2)\,\mathrm{Im}\, B_\rho(s_1)B_\rho(s_2)^*}{(m_\tau^2 + 2Q^2)\int ds_1 ds_2 (-V_1^2|B_\rho(s_2)|^2 - V_2^2|B_\rho(s_1)|^2 - 2V_1 V_2\, \mathrm{Re}\, B_\rho(s_1)B_\rho(s_2)^*)} \tag{4.7}$$

e^+e^- *experiments at energies significantly above the τ threshold:* The tau rest-frame cannot be fully reconstructed, $\vec{n}_\tau$ is not known and the moment as defined previously cannot be measured. However, one can still define a moment with respect to $\vec{n}_\perp(-\vec{n}_Q)\,\mathrm{sign}(s_1 - s_2)$ but now $-\vec{n}_Q = \vec{n}_L$ denotes the direction of the lab viewed from the 3π-rest frame.($\vec{n}_Q$ is again the direction of the hadrons in the lab system). After the replacement $\vec{n}_\tau \to \vec{n}_L$ the asymmetry can be defined as in (4.5) with $x \equiv Q^0_{lab}/E_{beam}$ fixed and one obtains

$$\langle \vec{n}_L \vec{n}_\perp \,\mathrm{sign}(s_1 - s_2)\rangle = -\gamma_{AV} \cos\psi A_{LR}(Q^2)$$

where $\cos\psi = \vec{n}_L \vec{n}_\tau = -\vec{n}_Q \vec{n}_\tau$ can be completely reconstructed and expressed in terms of the remaining kinematical variables.

$$\cos\psi = \frac{x(m_\tau^2 + Q^2) - 2Q^2}{(m_\tau^2 - Q^2)\sqrt{x^2 - 4Q^2/s}}$$

($s = 4E^2_{beam}$) Alternatively x could be expressed in terms of θ (which denotes the angle between the direction of flight of the τ in the lab frame and the direction of the hadronic system in the τ rest frame) through the relation

$$x = \frac{1}{2}\left[\left(1 + \frac{Q^2}{m_\tau^2}\right) + \left(1 - \frac{Q^2}{m_\tau^2}\right)\sqrt{1 - \frac{4m_\tau^2}{s}}\cos\theta\right] \tag{4.8}$$

In the limit $\beta \to 0$,i. e. when the taus are produced at threshold, $\vec{n}_L = \vec{n}_\tau$, $\cos\psi = 1$ and the previous result is reproduced.

The size of the parity violating asymmetry is evidently proportional to the relative size of vector vs. axial vector couplings at the lepton vertex and thus proportional to γ_{VA}. Although it depends crucially on the relative phase between the two $\rho\pi$ amplitudes in (3.5), the asymmetry depends only mildly on the exact form of the $\rho \to \pi\pi$ amplitude. To support this statement, the predictions resulting from a single ρ with constant width (153 MeV) and those for models 1 and 2 of table 1 are shown in Fig. 8.

The results are, however, quite sensitive to the specific form of the $a_1\rho\pi$ coupling $\epsilon_a\epsilon_\rho$ inherent in (3.5). Replacing this effective coupling by $(\epsilon_a q_1)(\epsilon_\rho q_1)$ which is equivalent to the amplitude denoted D-wave in [17], one finds

$$A_{LR}(Q^2) = \frac{9Q^2 \int ds_1 ds_2 \sqrt{(s_1 s_2 s_3 - m_\pi^2(Q^2 - m_\pi^2)^2)/Q^2}\,\mathrm{sign}(s_1 - s_2)\,\mathrm{Im}\,C_1 C_2^*}{(m_\tau^2 + 2Q^2)\int ds_1 ds_2(-W_1^2|C_2|^2 - W_2^2|C_1|^2 - 2W_1 W_2\,\mathrm{Re}\,C_1 C_2^*)} \tag{4.9}$$

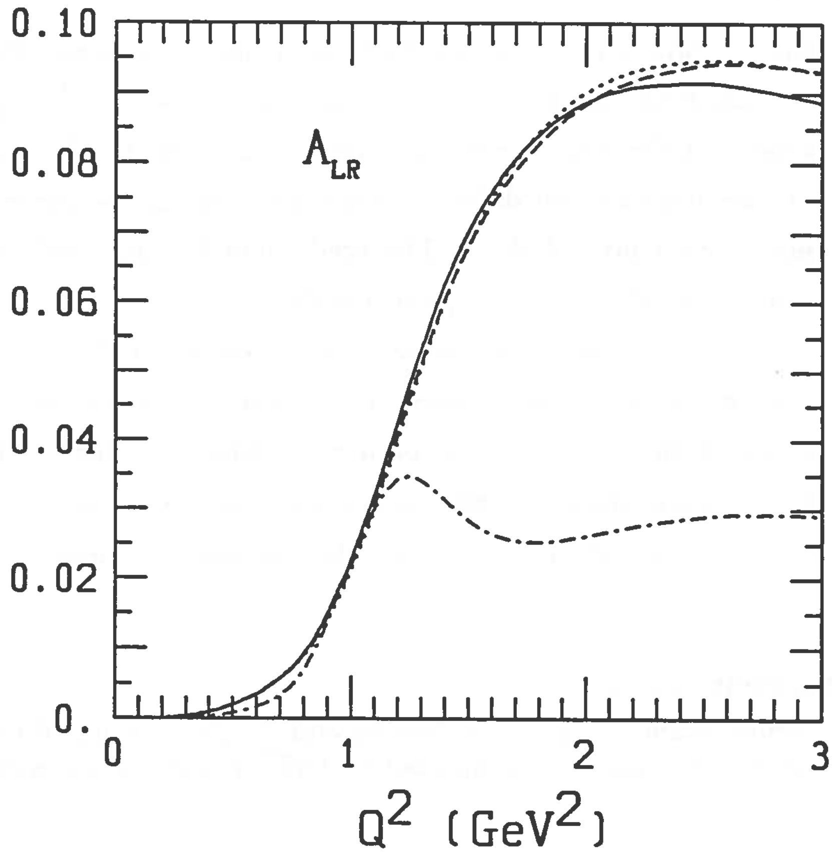

Fig. 8: The function $A_{LR}(Q^2)$ as defined in eq. (4.7) for different models of the ρ Breit Wigner (solid/dashed/dotted curves), and (dashed-dotted curve) for the "D-wave" amplitude (eq. (4.9)).

with

$$C_1 = (s_3 - s_2)B_\rho(s_1) \qquad C_2 = (s_3 - s_1)B_\rho(s_2)$$

$$W_{1\alpha} = (2V_{2\alpha} - V_{1\alpha}) \qquad W_{2\alpha} = (2V_{1\alpha} - V_{2\alpha})$$

which leads to a result drastically different as shown also in Fig. 8.

Summary

Semileptonic τ decays to two and three pions have been considered. Based on recent data for the pion form factor a new prediction for $\Gamma(\tau \to \nu\pi^-\pi^0)/\Gamma(\tau \to \nu e\bar{\nu}_e)$ of 1.32 ± 0.05 has been derived. The chiral model — supplemented by vector dominace — is used to predict rate and differential distributions for the three pion mode in good agreement with present data. The predictions for the total rate depend on the inclusion of the ρ' in the two pion distribution and on the incorporation of dispersive corrections. Differential distributions in the mass of the hadronic system and in the Dalitz plane are fairly insensitive towards details of the model and in good agreement with the data. The parity violating asymmetry which has been predicted theoretically and observed experimentally is studied and found to be fairly insensitive towards the details of the model for the hadronic decays.

Acknowledgements

The authors acknowledge H. Kolanoski and A. Pich for fruitful conversations. The work of A.S. was partially supported by CICYT under grant number AEN-89-0348.

REFERENCES

[1] M. Perl et al., *Phys. Rev. Lett.* **35** (1975) 1489.

[2] M. Perl, Rewiev presented at the XIV Lepton Photon Conf. Stanford 1989; C. Kiesling in High Energy Electron Positron Physics, eds. A. Ali and P. Söding, World scientific, Singapore, 1988,

[3] H.B. Thacker and J.J. Sakurai, *Phys. Lett.* **36 B** (1971) 103.

[4] Y.S. Tsai, *Phys. Rev.* **D 4** (1971) 2821.

[5] F.J. Gilman and D.H. Miller, *Phys. Rev.* **D 17** (1978) 1846; F.J. Gilman and S.H. Rhie, *Phys. Rev.* **D 31** (1985) 1066.

[6] R. Fischer, J. Wess and F. Wagner, *Z. Phys.* **C 3** (1980) 313.

[7] J.H. Kühn and F. Wagner, *Nucl. Phys.* **B 236** (1984) 16.

[8] L.M. Barkov et al., *Nucl. Phys.* **B 256** (1985) 365.

[9] ARGUS-Coll., preliminary results presented by A. Walther at the DPG-meeting, Hamburg, 23.3.1990.

[10] G.Gounaris and J.J. Sakurai, *Phys. Rev. Lett.* **21** (1968) 244.

[11] Z.Y. Fang, G. Lopez Castro and J. Pestieau, *Nuovo Cimento* **100** (1988) 155.

[12] M.G. Bowler, *Phys. Lett.* **182 B** (1986) 400.

[13] A. Pich, Proc. of the "Tau-Charm Factory" workshop. SLAC-343, Stanford, 1989, 416.

[14] V. Chabaud et. al, *Nucl. Phys.* **B 223** (1983) 1.

[15] Particle data group, *Phys. Lett.* **204 B** (1988) 1.

[16] B. Costa de Beauregard et al.,*Phys. Lett.* **67 B** (1977) 213; A. Quenzer et al., *Phys. Lett.* **76 B** (1978) 512.

[17] W.R. Frazer, J.R. Fulco and F.R. Halpern, *Phys. Rev.* **B 136** (1964) 1207.

[18] N.A. Thornquist, *Z. Phys.* **C 36** (1987) 695.

[19] ARGUS Coll., H. Albrecht et al., *Z. Phys.* **C 33** (1986) 7.

[20] H. Kolanoski, private communication.

[21] MAC Coll., H.R. Band et al.,*Phys. Lett.* **198 B** (1987) 297.